Journal of Integrative Agriculture 2026, 25(9): 3559–3571

Available online at ScienceDirect

Journal of Integrative Agriculture

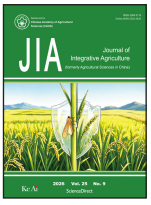

RESEARCH ARTICLE

Identification of novel QTLs contributing to resistance against *Aspergillus flavus* in maize (*Zea mays* L.) using an enlarged genotype panel

Jianxin Li[1], Lianglei Zhang[1], Xiang Guo[1], Jihong Zhang[1], Shiwei Wang[1], Xinyu Sun[1], Haiyang Duan[1], Huiling Xie[1], Dong Ding[1], Jihua Tang[1, 2#], Xuehai Zhang[1#]

[1] *National Key Laboratory of Wheat and Maize Crop Science/College of Agronomy, Henan Agricultural University, Zhengzhou 450046, China*
[2] *The Shennong Laboratory, Zhengzhou 450002, China*

Highlights

- Temperate inbreds showed greater resistance to *Aspergillus flavus* than tropical and subtropical materials.
- The identification of 13 novel QTLs using an enlarged genotype panel suggests that higher marker density enhances the statistical power of genome-wide association study.
- Inbreds with the favorable haplotype combination of the two genes (*elo1* and *ZmFUC1*) demonstrated significant resistance to *A. flavus*. Gene *ZmFUC1* was selected during the domestication of teosinte (*Zea mays* ssp. *mexicana*) into modern maize and during the adaptation from tropical/subtropical maize to temperate maize.
- Molecular markers in the promoter region of *ZmFUC1* can efficiently identify maize germplasm with beneficial haplotypes for resistance to *A. flavus*.

Abstract

Maize (*Zea mays* L.) is a crucial global crop that serves as a primary source of food and feed. However, its kernels are susceptible to infection by *Aspergillus flavus*, a fungus known for producing aflatoxins — which are highly carcinogenic compounds harmful to human and animal health. Identifying quantitative trait loci (QTLs) for aflatoxin resistance and developing aflatoxin-resistant maize varieties are essential for mitigating aflatoxin contamination. In this study, a genome-wide association study (GWAS) using an enlarged genotypic panel of 311 maize inbred lines was used to identify genetic loci associated with *A. flavus* resistance. Phenotypic data on *A. flavus* resistance were collected through controlled inoculation experiments conducted under controlled conditions. The results revealed that the resistance to *A. flavus* follows a normal distribution. In addition, temperate inbreds exhibited stronger resistance to *A. flavus* than tropical/subtropical materials. This study identified 13 novel QTLs encompassing 47 highly expressed genes, with each QTL explaining 8.22–27.71% of the phenotypic variation, indicating that the higher marker density improved statistical power. Gene Ontology (GO) enrichment and Kyoto Encyclopedia of Genes and Genomes (KEGG) pathway analyses revealed that these genes are related to fatty acid synthesis, glycoside decomposition, and root growth and development. One specific gene located on *ZmAFR16*, Zm*FUC1*, displayed clustered peaks and accounted for an average of 10.21% of the phenotypic variation. This gene was found to play a role in cell membrane formation and possess alpha-L-fucosidase activity, so it promotes glycoside metabolism and contributes to polysaccharide degradation. Haplotype analysis showed significant differences in resistance to *A. flavus* among the different haplotypes of *elo1* and Zm*FUC1*. Inbreds carrying the favorable haplotype combination of these two genes exhibited strong resistance to *A. flavus*. A select sweep analysis indicated that Zm*FUC1* was selected during the domestication of teosinte (*Zea mays* ssp. *mexicana*) to modern maize, as well as during the adaptation from tropical/subtropical maize to temperate maize. Importantly, this study developed molecular markers in the promoter region of Zm*FUC1* to efficiently identify maize germplasm with beneficial haplotypes for resistance to *A. flavus*. These findings not only enhance our understanding of the genetic factors influencing maize kernel resistance to *A. flavus* but also offer valuable insights for improving existing germplasm and developing new maize varieties with enhanced resistance to this pathogen.

Received 28 September 2024; Received in revised form 12 December 2024; Accepted 17 December 2024; Available online 3 January 2025
[#]Correspondence Xuehai Zhang, Tel: +86-371-56990188, Fax: +86-371-56990186, E-mail: xuehai85@126.com; Jihua Tang, E-mail: tangjihua1@163.com

doi: 10.1016/j.jia.2025.01.002

Keywords: maize, *Aspergillus flavus* resistance, genome-wide association analysis, mycorrhizal fungal symbiosis, fatty acid synthesis and elongation, XP-CLR

1. Introduction

Maize (*Zea mays* L.) is a crucial food and feed crop that significantly contributes to the national economy and people's livelihoods (Erenstein *et al.* 2022). However, it is vulnerable to *Aspergillus flavus*, a saprophytic fungus known for producing aflatoxin B1 (AFB1). This toxin, classified as a Group I carcinogen by the International Agency for Research on Cancer (IARC), increases the risk of liver cancer in humans (Eaton and Gallagher 1994). AFB1 poses substantial risks to humans, animals, and plant health (Hedayati *et al.* 2007; Amaike and Keller 2011; Cogliano *et al.* 2011). Peanuts and maize are among the primary hosts of *A. flavus* (Fu 2018). The aflatoxins in peanuts and maize are linked to 25,200 to 155,000 liver cancer cases annually (Liu and Wu 2010), highlighting the urgent need for effective control strategies to reduce food safety risks and economic losses. Current methods include agricultural practices such as crop rotation, resistant variety selection, and optimized fertilization. Biological control techniques, including probiotics and antagonistic microorganisms, along with chemical interventions like fungicides and detoxification agents, also play a key role in minimizing contamination (Yin *et al.* 2008; Caceres *et al.* 2020). Solar radiation has proven efficient for aflatoxin degradation, with sunlight treatment achieving a 75% reduction in AFB1 levels on contaminated peanuts after just 10 min (Herzallah *et al.* 2008). Other chemical methods, such as potassium sorbate, ultraviolet irradiation, and heating, can degrade aflatoxins but may negatively affect food quality and nutrition (Wang *et al*. 2016).

Recent biotechnological advances offer promising solutions, such as host-induced gene silencing (HIGS) to suppress the *aflC* gene in maize, which effectively inhibits aflatoxin production (Thakare *et al.* 2017). Previous studies have demonstrated that genes associated with aflatoxin-degrading enzymes can effectively reduce aflatoxin levels in maize (Schmidt *et al.* 2021). With the advancement of transgenic technology, BT maize has been developed to confer resistance to insects. Studies have indicated that planting BT maize can also effectively reduce the incidence of aflatoxin, making it a valuable strategy for mitigating aflatoxin contamination (Yu *et al.* 2024). In addition, the transfer of the *AttM* gene, identified through BLASTP comparison, into *E. coli* BL21 achieved degradation rates of 86.78% for AFB1, 81.32% for ochratoxin A, and 67.82% for zearalenone (Cheng *et al.* 2023). These integrated strategies are crucial for reducing aflatoxin risks while ensuring food safety and quality.

Several effective technologies have been developed for early aflatoxin detection, including high-performance liquid chromatography (HPLC) (Li T *et al.* 2021), thin layer chromatography (TLC) (Qu *et al.* 2018) and colloidal gold immunochromatography assay (GICA) (Shim *et al.* 2007). However, these methods have not fully addressed the issue of aflatoxin pollution. The most efficient and practical approach for reducing pre-harvest *A. flavus* contamination in maize remains the development of resistant lines (Baisakh *et al.* 2023). In maize, an F_2 population derived from the resistant inbred line H152 and the sensitive inbred line PI143 identified an *A. flavus* susceptibility gene on chromosome 2 at 0.80 cM from the *umc1992* marker, and an *A. flavus* resistant gene on chromosome 3, positioned 0.66 and 0.75 cM from the *umc2259* and *umc2174* markers, respectively (Ding 2016). Another study using an $F_{2:3}$ population from the resistant inbred line Mp313E and the susceptible inbred line B73 identified 13 QTLs associated with *A. flavus* resistance (Brooks *et al.* 2005). Similarly, crossing Mp313E with the susceptible variety Va35 led to the identification of 20 QTLs (Willcox *et al.* 2013), with only five QTLs common across these populations. Furthermore, through GWAS of 313 maize inbred lines, four QTLs associated with resistance to *A. flavus* were identified, which can be leveraged to develop new maize varieties with improved resistance (Han *et al.* 2020). Several meta-QTL (MQTL) studies, integrated with transcriptome data, have identified candidate causal QTLs/genes and linked markers associated with resistance to *A. flavus* in maize (Xiang *et al.* 2010; Mideros *et al.* 2014; Baisakh *et al.* 2023). These findings can support the marker-assisted breeding of *A. flavus*-resistant maize varieties.

Aspergillus flavus resistance is a complex quantitative trait influenced by multiple genes and environmental factors. Despite the advancements discussed above, elucidating the genetic mechanisms underlying this resistance holds significant promise for the development of high-quality and resistant crop varieties. This endeavor could substantially mitigate *A. flavus* contamination in crops such as maize and offer extensive benefits. Advances in high-throughput sequencing technology have revolutionized genetic studies, particularly with the development of higher-density SNP markers, which has significantly improved the statistical power and accuracy of gene localization in GWAS (Zhang *et al.* 2016). Building upon this progress, this study conducted an improved GWAS on maize *A. flavus* resistance phenotypes by leveraging ultra-high density molecular markers comprising 10.77 million SNPs (10.77M) and 21,081 polymorphic structural variations (pSVs). The objectives were to 1) explore the distribution of resistance levels in temperate and tropical maize inbred lines; 2) identify novel genetic loci and candidate genes associated with *A. flavus* resistance; and 3) develop molecular markers and quickly identify maize germplasm with superior haplotypes for *A. flavus* resistance. This study deepens our understanding of the genetic mechanisms underlying *A. flavus* resistance and provides valuable germplasm resources and theoretical foundations for the ongoing improvement of maize varieties that can prevent *A. flavus* infections.

2. Materials and methods

2.1. Phenotype resources

This study analyzed the phenotypes of 313 maize inbred lines by evaluating their resistance to *A. flavus* based on infection area grades. These 313 lines were randomly selected from a panel of 513 inbred lines used for association mapping (Yang *et al.* 2011; Li *et al.* 2012) and were categorized as follows: 22 inbred lines classified as stiff-stock (SS) subgroups with temperate origins, 84 inbred lines as non-stiff-stock (NSS) subgroups with temperate origins, 131 inbred lines as tropical and sub-tropical (TST) subgroups with tropical/subtropical origins, 70 inbred lines as mixed subgroups (Mixed), and unclassified subgroups. For the experiments on *A. flavus* infection, a comprehensive dataset detailing the resistance phenotypes based on the infection area grades among the maize inbred lines was obtained in a previous study (Han *et al.* 2020). Specifically, approximately 24 kernels from each inbred line were inoculated with *A. flavus* in a growth chamber. After 7 days of incubation, the resistance levels were assessed. The resistance phenotype of *A. flavus* is defined as:

$$\text{Infection area level}=\frac{\text{Infected area}}{\text{Total grain area}}\times 10$$

where the infected area refers to the extent of *A. flavus* infection on maize kernels after 7 days. To ensure data integrity, one duplicate maize inbred line, K12, was removed. To facilitate the GWAS analysis, 11 infection area grades (0–10) were defined based on the infection area levels (Han *et al.* 2020). Subsequently, 311 inbred lines remained eligible for further analyses, including general statistical analysis and the GWAS.

2.2. Genotype resources

An enlarged genotype dataset (B73 RefGen_v4), consisting of 10,771,042 SNPs (10.77M) of 505 lines and 21,081 pSVs of 516 lines based on the structural variation between B73, MO17 and SK, was employed for the GWAS in this study. This dataset, obtained through DNA deep resequencing (~20X) (Yang *et al.* 2019), provides high-density coverage of the entire maize genome. Since the reference genome version of this enlarged genotype differs from the previous genotype of 513 lines (B73 RefGen_v2, 558, 529 SNPs, 0.56M), CrossMap software (Zhao *et al.* 2014) was used to convert the positions of the 0.56M genotype dataset to the Maize B73 RefGen_v4 version. This conversion facilitated the comparison of the two GWAS results. Quality control for the genotype was performed with a minor allele frequency (MAF)>0.05 and a missing data ratio≤0.2. The relationships between the 505 and 513 lines, as well as between the 311 and 505 lines, are shown in Fig. 1-A. In addition, only 333,305 SNPs from the 0.56M dataset were included in the 10.77M SNPs (Fig. 1-B), mainly due to differences in SNP genotyping methods between the two datasets.

2.3. Genome-wide association analyses

GWAS was conducted using three models: the general linear model (GLM) with population structure (Q), the mixed linear model (MLM) with kinship (K), and the MLM with both population structure and kinship (Q+K). The Q matrix was obtained using the STRUCTURE software (V2.2), and K=3 was selected as the final result (Liu *et al.* 2016). The kinship matrix was calculated using the method described in Loiselle

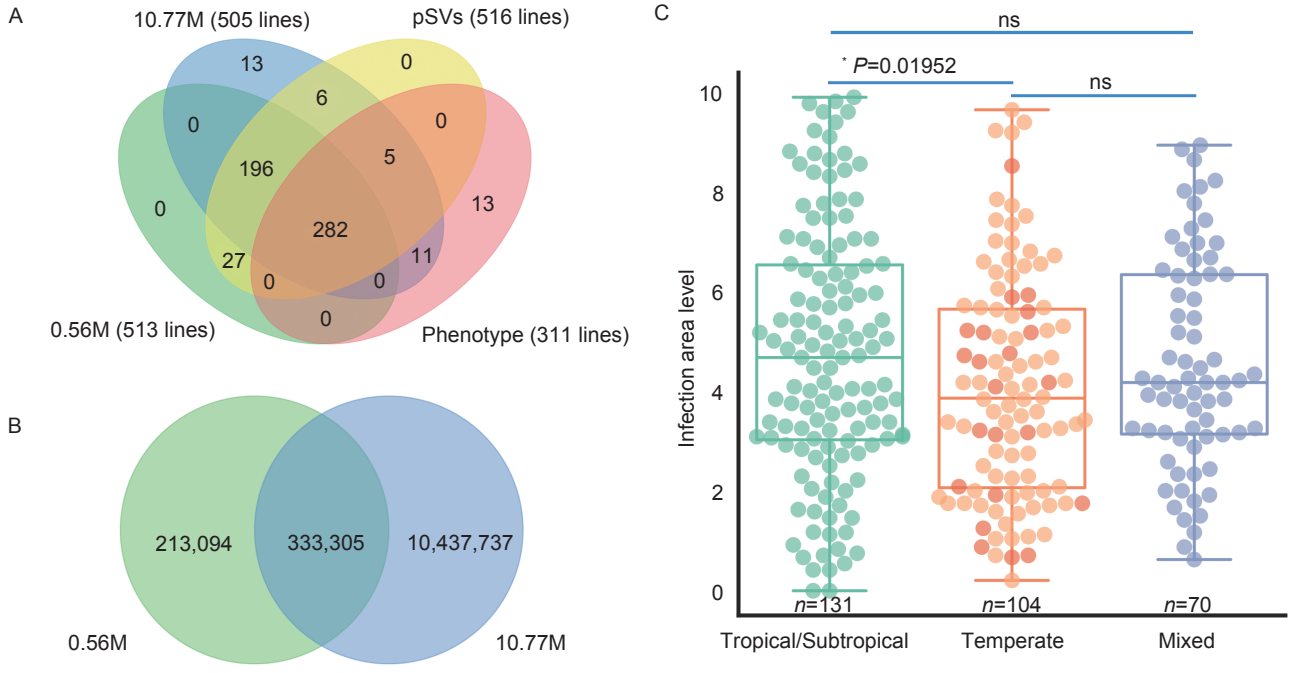

Fig. 1 Comparison of *Aspergillus flavus* infection area levels among different maize subgroups and their different genotypes. A, comparison of maize inbred lines based on different genotypes or phenotypes. B, comparison of SNPs between the two datasets (0.56M *vs.* 10.77M). C, comparison of *A. flavus* infection area levels among temperate, tropical/subtropical, and mixed maize groups. In the temperate group, dark orange dots represent stiff-stock (SS) maize lines, and light orange dots represent non-stiff-stock (NSS) maize lines. * indicates significance at $P<0.05$ (Student's *t*-test, one-tailed); ns, non-significant.

et al. (1995). These models were implemented in TASSEL 5.2.81 to test the relationships between SNPs and infection classes.

SNPs defined as significant SNPs with a *P*-value≤2.04×10^{-6} in the GWAS results were used for the common GWAS threshold lines. Due to the low density of the pSVs dataset, its threshold line was lowered to 1.0×10^{-4}. A significant SNP upstream and downstream in the 50 kb range was defined as a QTL. The genes within each QTL were considered candidate genes (Li W *et al.* 2021). Quantile-quantile (QQ) and Manhattan plots were generated using the "CMplot" package in R 4.3.1 (Yin *et al.* 2021).

2.4. Candidate gene analyses

Genes located within a ±50 kb range of significant SNP physical positions, based on a linkage disequilibrium (LD) threshold of 50 kb, were extracted using the maize B73 (RefGen_v4) reference genome (Li W *et al.* 2021). Gene function and annotation information were obtained by querying databases such as NCBI (www.ncbi.nlm.nih.gov/), UniPort (https://www.uniprot.org/), Gramene (https://www.gramene.org/), EnsemblPlants (http://plants.ensembl.org/), and MaizeGDB (https://www.maizegdb.org/). Furthermore, homologous gene annotation information was retrieved from various databases including TAIR (https://www.arabidopsis.org/) and the National Rice Data Center (http://www.ricedata.cn/).

2.5. GO and KEGG analyses

Based on the B73 kernel gene expression data for 20 days after pollination (B73_Embryo_20_DAP), genes with expression levels within the QTL were selected, and expression data were obtained from the ZEAMAP (Gui *et al*. 2020). These genes were converted to the B73 RefGen_v4 version using MaizeGDB. For further functional characterization, GO enrichment and KEGG pathway analyses were conducted using the OmicShare Tools (https://www.omicshare.com/tools).

2.6. Haplotype analysis

SNPs from all exons within the identified candidate genes were extracted using the Pandas library in Python. Different haplotypes were defined based on the nucleotide sequences of the extracted SNPs within the association population. To ensure accuracy, SNPs with missing data and haplotypes with fewer than 30 inbred lines were excluded from this analysis. Phenotypic analysis was conducted based on the identified haplotypes. The Student's *t*-test was performed using Microsoft Excel 365 to compare phenotypic differences among haplotypes. Boxplots were generated using the "Seaborn" package in Python to visualize the distribution of phenotypes across different haplotypes.

2.7. Select sweep analysis

XP-CLR (Chen *et al.* 2010) is a method that uses likelihood ratio tests to detect genomic differences between two populations due to selection. Data for 81 teosinte (Mexicana) and 505 modern maize inbred line genotypes (Chen *et al*. 2022) were downloaded using XP-CLR software (version1.1.2, size=1,000, step=1,000, maxsnp=100) to choose a clear analysis. The top 10% of the xpclr value was defined as the selective peak, and the gene nearest to the selective peak was the selected gene.

2.8. Construction of the phylogenetic tree

To enhance the credibility of *Zm00001d021197*, designated as *ZmFUC1*, the sequences and its homologous genes in *Arabidopsis*, rice, barley, wheat, lettuce, soybean, sugar beet, cabbage, sesame, potato, sorghum, pineapple, and chili were retrieved from Gramene (https://www.gramene.org/). These sequences were aligned using the neighbor-joining method in MEGA 11 software, and the resulting phylogenetic tree was visualized using iTOL (https://itol.embl.de/).

2.9. Development of molecular markers

A notable insertion-deletion (InDel) region of approximately 855 bp was found in the promoter region of the *Zm00001d021197* gene (1,220 bp upstream of the ATG start codon). Primers targeting this region were developed using the NCBI Primer-BLAST tool and validated for specificity with BLASTN. The availability of InDel marker primers was determined *via* agarose gel electrophoresis, and the DNA of 311 associated populations was extracted for PCR amplification. The haplotype analysis was conducted based on the band type, and the ability of the marker to judge the resistance to *A. flavus* was verified by the Student's *t*-test.

3. Results

3.1. Significant differences in resistance to *A. flavus* among maize subgroups

A general statistical analysis was conducted on the *A. flavus* resistance phenotype of 311 maize inbred lines. Resistance was quantified based on the infected area, which represents the extent of *A. flavus* infection on maize kernels after 7 days, so a smaller infected area indicates greater resistance. The analysis revealed infection area levels ranging from 0 to 9.88 (Table 1), indicating substantial phenotypic variability. To investigate the aflatoxin resistance among different maize subgroups, the 311 inbred lines were divided into tropical/subtropical, temperate, and mixed groups for statistical analysis. Notably, the temperate maize group exhibited stronger resistance to *A. flavus* than the tropical/subtropical group (Fig. 1-C).

3.2. Larger genotypic panels improve the statistical power of GWAS

The choices of GWAS model and single nucleotide polymorphism (SNP) density significantly impact the GWAS results. A previous study assessed resistance to *A. flavus* by calculating the ratio of infected area to surface area (infection area level) in 313 maize inbred lines and used the GLM model for GWAS (Han *et al.* 2020). With advances in high-throughput sequencing technology (NGS), increasing numbers of SNPs and pSVs have been identified, and they provide more comprehensive genetic information. To determine whether a greater marker density improves the

Table 1 Descriptive statistics for resistance to *Aspergillus flavus* in the maize association mapping population

Trait	Observations	Range	Average	Median	Mode	Variance	SD	Kurtosis	Skewness
Infection area level	311	0–9.88	4.48	4.17	4.17	5.55	2.36	–0.64	0.33

statistical power of GWAS for identifying *A. flavus* resistance loci, this study used two genotype datasets: one with 10,771,042 (10.77M) high-quality SNPs and another with 21,081 pSVs, based on the structural variation between B73, MO17, and SK (Yang *et al.* 2019). GWAS was re-conducted using both GLM and MLM models in the 311 maize inbred lines. The MLM model struggled to control false negatives compared to previous studies (Appendix A). Consequently, the GLM model was chosen for the final GWAS analysis (Fig. 2).

A total of 37 significant SNPs were newly identified within 15 QTLs, explaining phenotypic variations ranging from 8.22 to 27.71% (Appendix B). Compared to previous GWAS results (using 0.56M SNPs, which detected 11 significant SNPs within six QTLs; Fig. 2-A), it is noteworthy that two QTLs were detected repeatedly. In chromosome 1, the interval between *ZmAFR1* (0.56M) and *ZmAFR1* (10.77M) is 1.47 Mb and the interval between *ZmAFR2* (10.77M) and *ZmAFR3* (10.77M) is 0.34 Mb. In chromosome 2, the interval between *ZmAFR4* (0.56M) and *ZmAFR5* (10.77M) is 0.31 Mb and the intervals between *ZmAFR8* (10.77M), *ZmAFR9* (pSVs), and *ZmAFR10* (10.77M) are 2.29 and 2.56 Mb. In chromosome 7, the interval between *ZmAFR13* (10.77M) and *ZmAFR14* (pSVs) is 2.88 Mb. This suggests that increasing the genotype density can enhance the statistical power of GWAS results. In addition, four QTLs detected by the pSVs dataset were not identified by the 10.77M SNP panel, including *Zm00001d006873*, which explained 16.85% of the phenotypic variation. Its homologous gene, *AT1G65870*, is involved in the disease resistance response.

Notably, the newly detected QTL on chromosome 7 (*ZmAFR16*) shows clustered peaks in the Manhattan plot, explaining an average of 10.21% of the phenotypic variation. Five significant SNP are included within *ZmAFR16*, highlighting this region as a critical interval. Moreover, *ZmAFR16* contains only two genes, *Zm00001d021197* and *Zm00001d021198*. Among them, *Zm00001d021197* is highly expressed in the seed coat and primary root of maize seeds (Walley *et al.* 2016). It is annotated as α-L-fucosylase, a member of the glycoside hydrolase family 29 (GH29) involved in glycoside degradation metabolism (de la Torre *et al.* 2002; Kato *et al.* 2018). In addition, α-L-fucosylase is found in the mucus secreted by maize and *Arabidopsis* seeds, where it decomposes mucopolysaccharides for microbial utilization (Nazari 2021). Beyond its potential role in conferring resistance to *A. flavus*, α-L-fucosylase also regulates the microbial community. This discovery provides valuable insights into the genetics of maize resistance to *A. flavus* infection, which was not previously detected in low-density genotypes. To comprehensively explore the genetic mechanism of maize resistance of *A. flavus*, 75 genes within the new 15 QTLs were screened. Based on the expression data of B73 kernels (B73_Embryo_20_DAP; Appendix C), genes that were not expressed were excluded, which left 47 genes with expression activity during this period. To pinpoint candidate genes, their annotations and homologs were cross-referenced through MaizeGDB, NCBI, TAIR (https://www.arabidopsis.org), Rice (https://www.ricedata.cn/gene/), and other relevant databases (Table 2).

3.3. GO and KEGG analyses

To better understand the functions of these genes, GO and KEGG analyses were performed on the 47 genes expressed in kernels (Fig. 3-A; Appendix D). The GO analysis revealed 21 genes in 94 terms (*P*-value<0.05). The top 32 GO terms (*P*-value<0.01) were primarily enriched in fatty acid synthesis and elongation (seven terms, two genes: *Zm00001d033637* and *Zm00001d045027*), glycoside metabolism (four terms, one gene: *Zm00001d021197*), formate metabolic (three terms, one gene: *Zm00001d006874*), and root development (two terms, two genes: *Zm00001d006756* and *Zm00001d018954*). The KEGG pathway analysis showed that 10 genes were enriched in 18 pathways (Fig. 3-B; Appendix E), with two pathways having significant *P*-values (*P*-value<0.05), involving two genes. *Zm00001d021197* was enriched in glycan degradation pathways, and *Zm00001d045027* in biotin metabolism, fatty acid biosynthesis, and metabolism pathways, consistent with the GO enrichment results. *Zm00001d033654* was also identified as participating in the MAPK signaling pathway and plant-pathogen interaction pathway, directly reflecting the resistance of maize to *A. flavus*. Notably, these genes are highly expressed in maize kernels, consistent with the infection site of *A. flavus* in our experiment.

3.4. Haplotype and select sweep analyses

Combining the candidate genes selected above for haplotype analysis (Fig. 4), significant differences in the resistance to *A. flavus* were found between the different haplotypes of *Zm00001d033637* and *Zm00001d021197*. For *Zm00001d021197*, 25 SNPs were identified (Fig. 4-C and E; Appendix F), including one SNP in the 5′UTR, six SNPs in the 3′UTR, four SNPs in the intron and 14 SNPs in the exon. Based on the exon SNP differences, the two haplotypes of HapA and HapB were identified, and 88 inbred lines belong to the optimal haplotype HapA. A total of 61 materials belong to HapB, where two SNPs are mutations from CC to AG. At the protein level, these two SNPs do not lead to amino acid changes, suggesting that the SNPs may affect translation efficiency resulting in phenotypic differences, or they may serve as molecular markers linked to variant sites. LD block analysis revealed a significant difference peak around 1,400 bp upstream of the gene, indicating potential differences in the promoter region. In addition, pan-genomic data showed that eight inbred lines overlapped with the associated population (Appendix G), with six belonging to HapA and two to HapB. Promoter sequence analysis revealed that HapB has an approximately 885 bp insertion around 1,220 bp upstream of

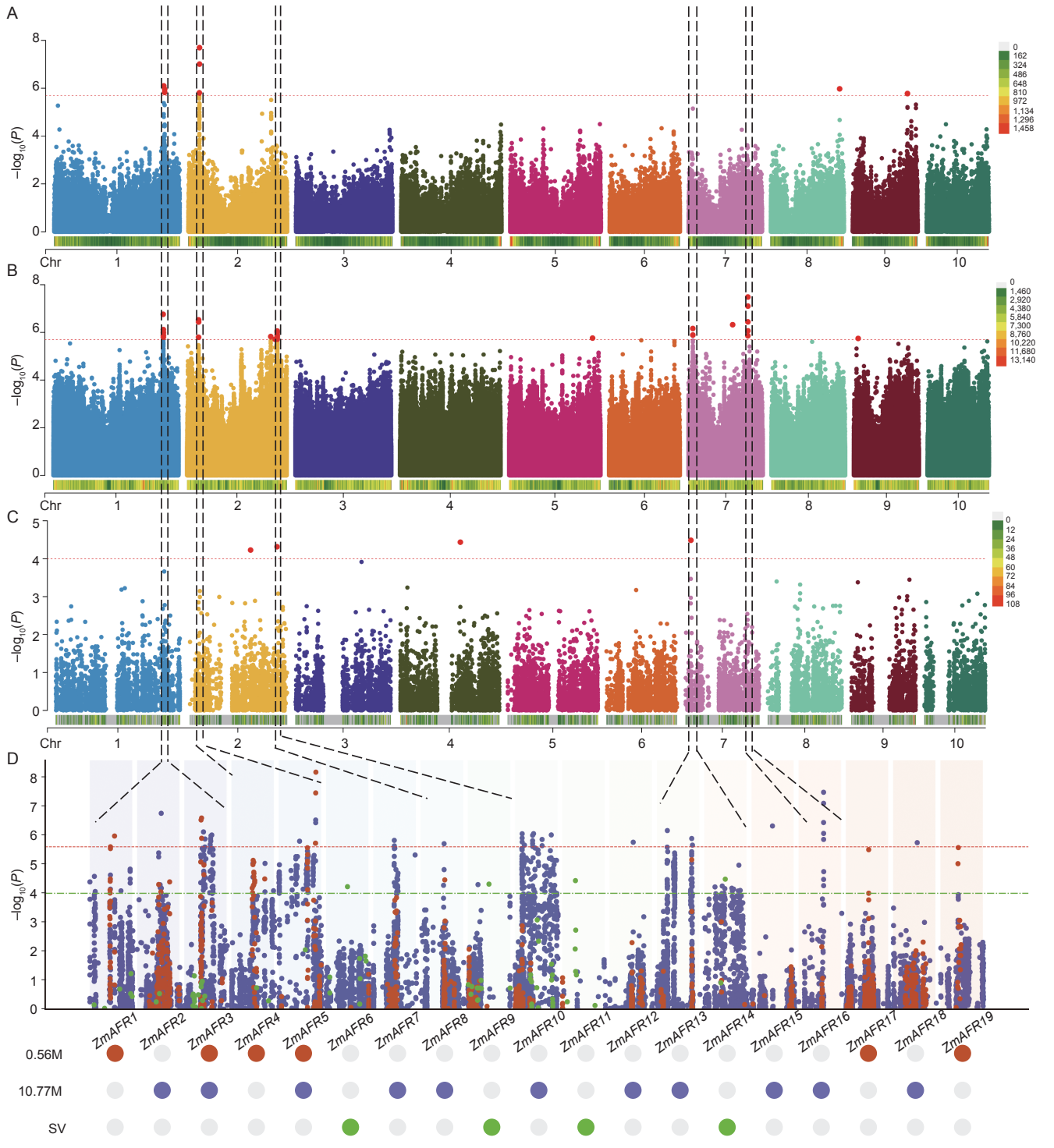

Fig. 2 Genome-wide association study (GWAS) results for the three sets of genotypes. A, Manhattan plot of the 0.56M dataset using the Q model, with a significance threshold of $P \leq 2.04\times10^{-6}$. B, Manhattan plot of the 10.77M dataset using the Q model, with a significance threshold of $P \leq 2.04\times10^{-6}$. C, Manhattan plot of the structure variation (pSVs) dataset using the Q model, with a significance threshold of $P \leq 1.0\times10^{-4}$. D, Manhattan plot showing 16 QTLs, with each block representing a distinct QTL. Below, an UpSet plot displays the QTL results for the three genotype datasets. Colored dots indicate the presence of significant SNPs or pSVs within the corresponding QTL for each genotype, while gray dots indicate their absence.

ATG, likely affecting promoter efficiency. Moreover, significant SNPs identified by GWAS are within this range.

For *Zm00001d033637* (designated as *eol1*), 11 SNPs were identified, all located on exons (Fig. 4-A; Appendix H), which could be divided into two haplotypes. Among them, 106 inbred lines belong to the optimal haplotype HapA, and 30 inbred lines belong to HapB. There are three SNP differences between these two haplotypes, and a key SNP with a transition from T to C at chr1.S_269339463 results in an amino acid change from Asn to Ser. Haplotype analysis

Table 2 Candidate genes identified by genome-wide association study and their functional annotations related to resistance to *Aspergillus flavus* in maize

QTL	Chr	Peak SNP	*P*-value	R^2 (%)	Gene	Function annotation
ZmAFR2	1	chr1.s_269328769	1.74E–07	9.70	*Zm00001d033632*	ARM repeat superfamily protein
					Zm00001d033633	Haloacid dehalogenase-like hydrolase (HAD) superfamily protein
					Zm00001d033634	Whole genome shotgun sequence of line PN40024 scaffold_151. assembly12× (fragment)
					Zm00001d033635	Cytidine/deoxycytidylate deaminase family protein
					Zm00001d033637	GNS1/SUR4 membrane protein family
					Zm00001d033640	DUF1764 domain protein
ZmAFR3	1	chr1.s_269774238	7.65E–07	8.76	*Zm00001d033654*	o10; opaque endosperm10: like o1
					Zm00001d033655	Mitogen-activated protein kinase kinase kinase 1
					Zm00001d033657	Histone acetyltransferase type B catalytic subunit
ZmAFR5	2	chr2.s_28087586	2.98E–07	9.52	*Zm00001d002954*	Cox19-like CHCH family protein
					Zm00001d002956	Endosomal targeting BRO1-like domain-containing protein
ZmAFR7	2	chr2.s_205081083	1.5E–06	8.47	*Zm00001d006342*	Mo-molybdopterin cofactor sulfurase
					Zm00001d006343	Carbohydrate-binding X8 domain superfamily protein
					Zm00001d006344	Protein SUPPRESSOR OF FRI 4
ZmAFR8	2	chr2.s_215957595	1.95E–06	9.13	*Zm00001d006753*	Indole-3-acetic acid amido synthetase
					Zm00001d006754	Zinc finger protein 1
					Zm00001d006756	WPP domain-containing protein 2
ZmAFR9	2	chr2_216604896_ 216604895_insertion_215	4.84E–05	18.23	*Zm00001d006873*	Disease resistance response protein-like; protein
					Zm00001d006874	F-box only protein 13
					Zm00001d006875	alt10; alanine aminotransferase10: putative alanine aminotransferase weakly expressed in seedling leaf
					Zm00001d006877	Formate dehydrogenase chloroplastic/mitochondrial
ZmAFR10	2	chr2.s_221091494	8.81E–07	8.64	*Zm00001d007053*	Got1/Sft2-like vesicle transport protein family
					Zm00001d007058	Protein Mo25
					Zm00001d007059	COX VIIa-like protein
					Zm00001d007060	E3 ubiquitin-protein ligase SP1
					Zm00001d007062	SNARE associated Golgi protein family
ZmAFR12	5	chr5.s_204541683	1.74E–06	8.22	*Zm00001d017699*	Probable xyloglucan endotransglucosylase/hydrolase protein 30
					Zm00001d017700	Lysine-specific demethylase REF6
ZmAFR13	7	chr7.s_10474577	6.88E–07	8.83	*Zm00001d018954*	Rhicadhesin receptor
					Zm00001d018955	Receptor-like cytosolic serine/threonine-protein kinase RBK1
					Zm00001d018957	60S ribosomal protein L4-1
ZmAFR15	7	chr7.s_108283105	4.77E–07	9.04	*Zm00001d020348*	Unknown function
ZmAFR16	7	chr7.s_145653183	3.28E–08	11.52	*Zm00001d021197*	Alpha-L-fucosidase 1
ZmAFR18	9	chr9.s_10630126	1.79E–06	8.35	*Zm00001d045027*	3-oxoacyl-[acyl-carrier-protein] synthase I chloroplastic
					Zm00001d045028	Nucleolar GTP-binding protein 1
					Zm00001d045029	Adrenodoxin-like protein 2 mitochondrial

(Fig. 4-B) showed significant differences between the two groups, indicating that amino acid changes may influence resistance to *A. flavus*.

Comparing the haplotypes of these two genes (Fig. 4-D), the inbred lines with both optimal haplotypes (AA) exhibited significantly higher resistance to *A. flavus* than other combinations of only one optimal haplotype (AB) or no optimal haplotype (BB). This suggests that these two genes work together to confer resistance to *A. flavus* infection.

Among the inbred lines in HapA of *Zm00001d033637* and HapA of *Zm00001d021197*, 41 inbred lines in the association mapping population shared these two excellent haplotypes. These materials offer valuable insights and theoretical guidance for breeding new maize varieties with enhanced resistance to *A. flavus*.

Selection and domestication analysis (XP-CLR) plays a crucial role in revealing the genetic basis of domestication processes in plants and animals. This method allows researchers to identify genomic regions that have undergone selective pressures during domestication, thereby shedding light on the genetic mechanisms underlying key domestication traits. To determine whether *Zm00001d021197* was selected during domestication, a select sweep analysis between 81 teosinte (*Zea mays* ssp. *mexicana*) and 505 maize materials was conducted using the XP-CLR method (Fig. 5-A). The clearance analysis revealed a peak (xpclr value=56.68) closest to *Zm00001d021197*. Calculating the nucleotide diversity (π value) across the gene (Fig. 5-B) showed similar diversity between *Zea mays parviglumis* and maize, but a noticeable difference between *Zea mays* ssp. *mexicana* and maize. Furthermore, the InDel within the promotor of *Zm00001d021197* was selected between the temperate and tropical/subtropical maize lines (Fig. 5-C). This suggests that *Zm00001d021197* was selected during the domestication of teosinte (*Zea mays* ssp. *mexicana*) into modern maize, as well as during the adaptation from tropical/subtropical maize to temperate maize. Next, the amino acid sequences of *Zm00001d021197* and its homologous genes were used

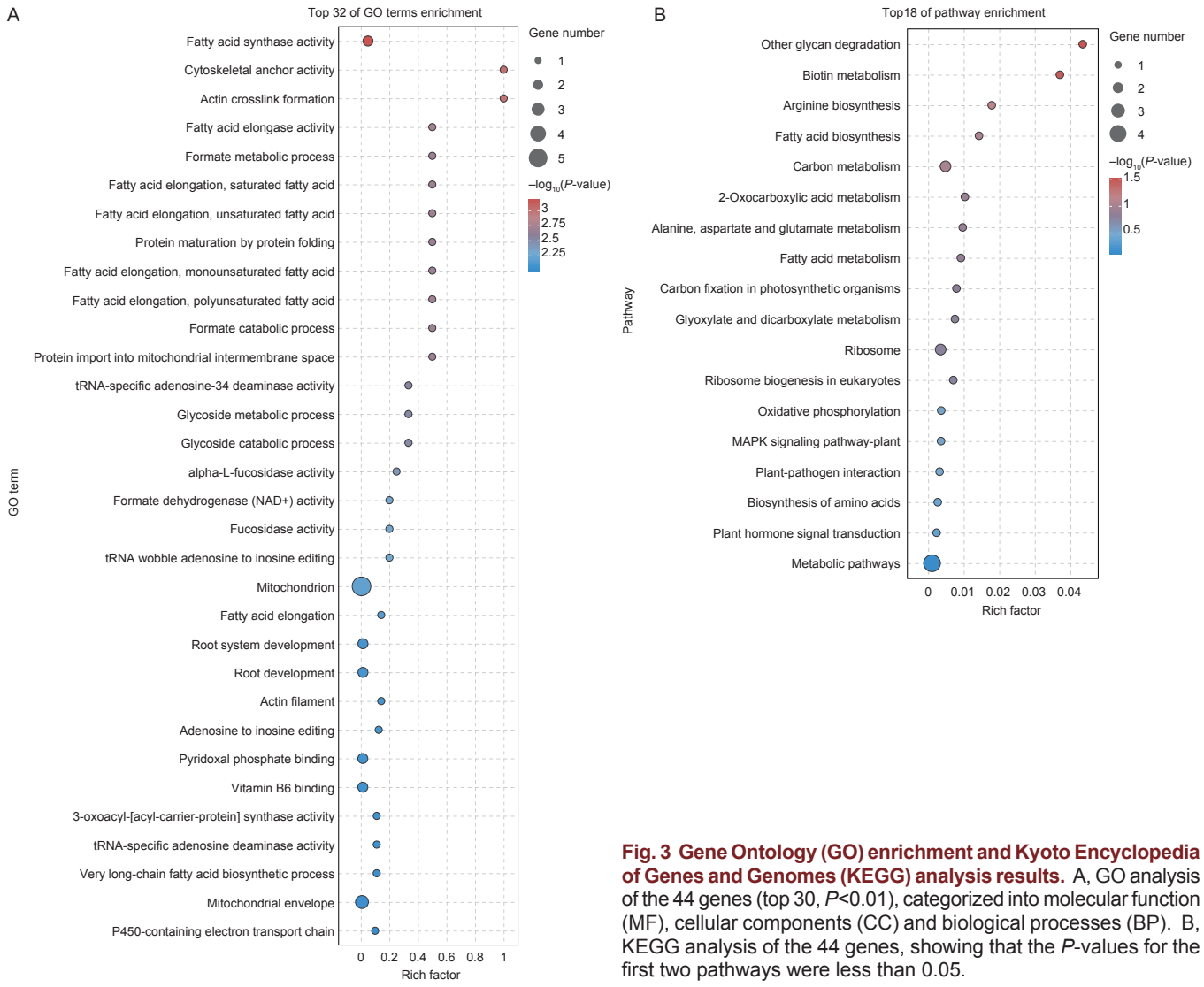

Fig. 3 Gene Ontology (GO) enrichment and Kyoto Encyclopedia of Genes and Genomes (KEGG) analysis results. A, GO analysis of the 44 genes (top 30, P<0.01), categorized into molecular function (MF), cellular components (CC) and biological processes (BP). B, KEGG analysis of the 44 genes, showing that the P-values for the first two pathways were less than 0.05.

to construct a phylogenetic tree using the Neighbor-Joining method (Fig. 5-D). The results showed that this gene is highly homologous to those in lettuce and *Arabidopsis,* and we named it *FUC1* since it encodes alpha-L-fucosidase 1, which is involved in the glycoside metabolism process.

3.5. Molecular marker development

Molecular markers can significantly enhance breeding efficiency. To effectively screen for varieties with high resistance to *A. flavus*, a pair of molecular markers targeting the promoter region of *Zm00001d021197* were developed. The target fragment was isolated using 1% agarose gel electrophoresis (Appendix I), and a polymorphism difference was found in this marker (Fig. 6-B). Then among eight randomly selected extreme haplotypes (four HapA and four HapB), all the HapA materials were lower bands, and all the HapB materials were upper bands (Fig. 6-C).

To verify the classification of the marker in the associated population, this pair of primers was used to validate the associated population (Appendix J). The results of the strip classification and haplotype analysis showed that the differences between haplotypes are significant (Fig. 6-A; P=0.04). To verify whether this marker can be applied in production practice, Zhengdan 958, MY73 and their parents (T1932 and T856 for MY73; Zheng 58 and Chang7-2 for Zhengdan 958) were examined (Fig. 6-D), and the results indicated that there was an insertion allele in T856 (the father of MY73), suggesting that MY73 would have weaker resistance to *A. flavus* compared with Zhengdan 958. This result confirms that *Zm00001d021197* effectively regulates resistance to *A. flavus*. The developed markers can be used for the rapid screening of resistant inbred lines or varieties, which is a substantial contribution to improving breeding efficiency. The implementation of these molecular markers will not only facilitate the quick identification of resistant genotypes but also strengthen the overall breeding strategy aimed at reducing aflatoxin contamination in maize.

4. Discussion

4.1. Comparison of *A. flavus* resistance among different subgroups

Aspergillus flavus is a fungal disease that severely impacts maize yield and quality, primarily through the production of aflatoxin, which is a secondary metabolite with potent

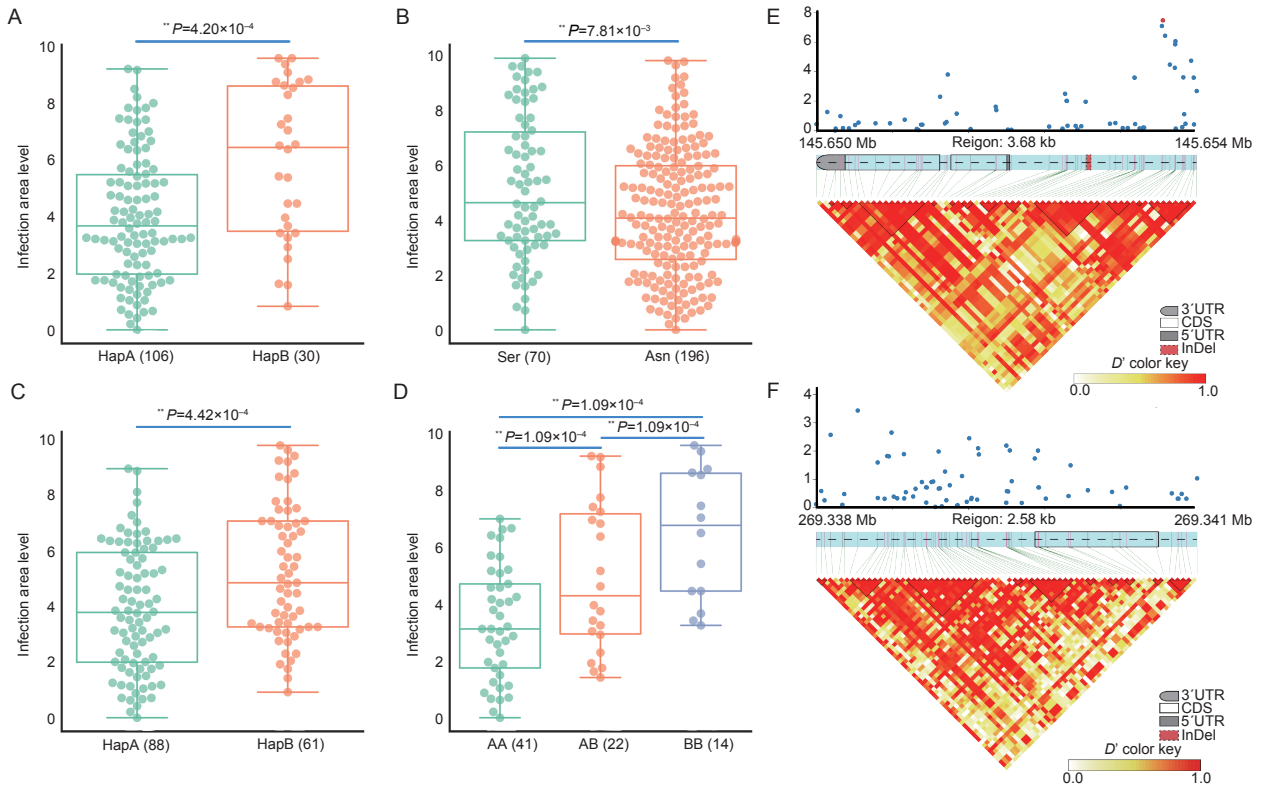

Fig. 4 Haplotype analysis results. A, haplotype analysis based on exons in *Zm00001d033637*, with material quantities of 106 for HapA and 30 for HapB. B, haplotype analysis based on non-synonymous mutation sites in *Zm00001d033637*, showing material quantities of 74 for Ser and 196 for Asn. C, haplotype analysis based on exons in *Zm00001d021197*, with material quantities of 88 for HapA and 61 for HapB. D, haplotype analysis based on the optimal number of haplotypes for the two genes mentioned above. AA represents materials with both optimal haplotypes (41 lines), AB represents materials with one optimal haplotype (22 lines), and BB represents materials with zero optimal haplotypes (14 lines). ** indicates $P<0.01$ (Student's *t*-test, one-tailed). E, linkage disequilibrium analysis of *Zm00001d021197*. F, linkage disequilibrium analysis of *Zm00001d033637*.

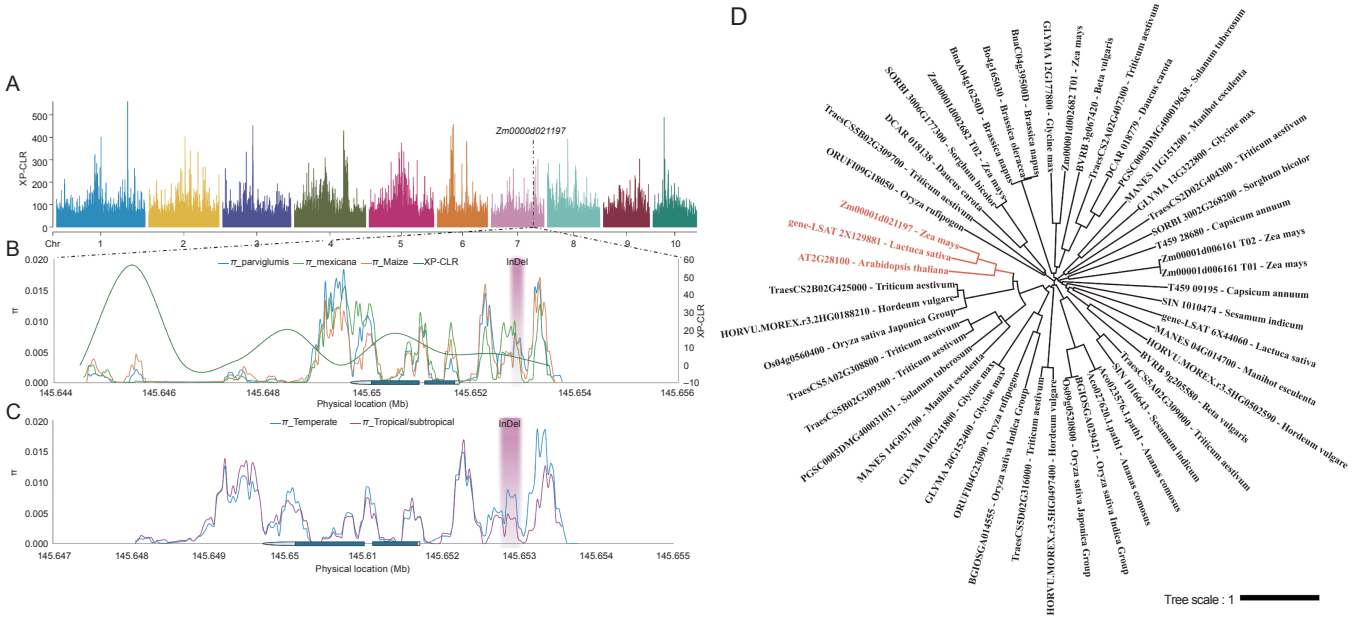

Fig. 5 Select sweep analysis and phylogenetic tree of *Zm00001d021197*. A, select sweep analysis across the entire genome for teosinte (*Zea mays* ssp. *mexicana*) and maize. B, nucleotide diversity and selection sweep analysis of *Zm00001d021197* (Chr7: 145,648,289–145,653,201) in teosinte (*Zea mays* ssp. *mexicana* and *Zea mays* ssp. *parviglumis*) and maize. C, nucleotide diversity analysis of *Zm00001d021197* (Chr7: 145,648,289–145,653,201) between tropical/subtropical maize and temperate maize. D, phylogenetic tree of *Zm00001d021197* and its homologous protein-coding genes.

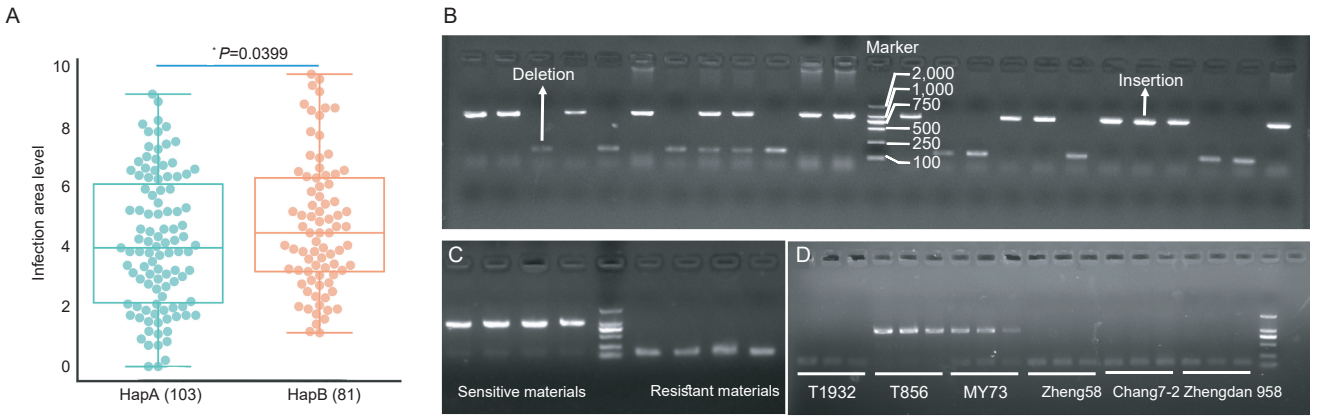

Fig. 6 Haplotype analysis and gel electrophoresis results using the developed marker. A, association mapping panel classified according to InDel markers, with HapA representing InDel-missing materials and HapB representing InDel-inserted materials. The material quantities for HapA and HapB were 103 and 81, respectively. B, polymorphism detected using a pair of primers, with polymorphism observed in the promoter region of *Zm00001d021197*. C, eight extreme haplotypes (4 HapA and 4 HapB) were randomly selected for verification. HapA materials showed all smaller bands, while HapB materials showed all larger bands. D, gel electrophoresis analysis using a specific pair of markers clearly distinguished the resistances in MY73, Zhengdan 958 and their parents (T1932 and T856 for MY73; Zheng 58 and Chang7-2 for Zhengdan 958). MY73 exhibits an InDel heterozygous insertion, while Zhengdan 958 does not. * indicates $P<0.05$ (Student's *t*-test, one-tailed).

carcinogenic and immunosuppressive properties. Understanding the genetic mechanisms of maize resistance to *A. flavus* is crucial for developing high-resistance varieties, leveraging resistance gene resources, and controlling this pathogen. This study analyzed 311 maize inbred lines by evaluating their resistance to *A. flavus* based on infection area grades (Han *et al.* 2020). Significant differences in resistance levels were observed among various subgroups, with temperate materials exhibiting significantly higher resistance than tropical/subtropical materials. This difference likely arose from maize's evolution after being introduced from tropical to temperate regions, where it developed stronger resistance to aflatoxin-producing fungi. Over time, these germplasms may have acquired natural resistance genes or mechanisms, such as enhanced antioxidant activity, which can help to provide better protection against fungal infections.

4.2. A larger genotype dataset effectively boosts the statistical power of GWAS

GWAS is an effective gene mapping method that is widely used for analyzing the genetics of human diseases and complex traits in plants and animals. Despite the known impact of *A. flavus* on maize, its genetic mechanism remains unclear. With the advent of high-throughput sequencing, ultra-high density SNP markers have become available. For the GWAS, this study used an enlarged genotypic panel and two genotypic datasets, including 10.77 million SNPs and 21,081 pSVs, combined with three statistical models (GLM+Structure, MLM+Kinship, and MLM+Structure+Kinship models, denoted as the Q, K, and Q+K models, respectively). The analysis effectively controlled for false positives, with the Q model showing the best performance. This GWAS identified 15 QTLs, with 13 being newly detected due to the enlarged genotype dataset. Only two QTLs overlapped with previous studies (0.56M), likely due to differences in sequencing methods, reference genome versions, and marker linkage degrees. Further analysis of the three genotypes revealed that four QTLs were sufficiently close to regard them as a single region. Nevertheless, the expanded markers exhibited significant statistical power.

4.3. Analysis of candidate genes

Notably, the significant cluster peak on chromosome 7, which corresponds to the QTL (*ZmAFR16*), underscores the substantial contribution of the *Zm00001d021197* gene to *A. flavus* resistance. The genes included in the other QTLs were then analyzed. *ZmAFR3* and *ZmAFR5*, which were focal points in previous studies, are identified here as hotspots, collectively containing five genes with significant expression levels. *Zm00001d033655* is annotated as Mitogen-Activated Protein Kinase Kinase Kinase 1 (MAPKKK1), a key component of the mitogen-activated protein kinase (MAPK) cascade system. The MAPK signaling pathway plays a crucial role in transmitting environmental and developmental signals in plants. It is activated in response to both abiotic (e.g., wind, rain, hail) and biotic (e.g., insect feeding) stressors, and triggers downstream defense responses (Sözen *et al.* 2020). *Zm00001d002954* is annotated as a Cox19-like CHCH family protein, and its *Arabidopsis* homolog AT3G06310 responds to geminivirus infection (Ascencio-Ibanez *et al.* 2008). GO annotation suggests that this protein may be involved in mitochondrial electron transfer, specifically the transfer of NADH to ubiquinone.

The remaining nine QTLs newly detected using an enlarged SNP panel (10.77M), comprise 38 differentially expressed genes. Among these, *Zm00001d033632* is annotated as an ARM repeat superfamily protein, while *Zm00001d033635* is a Cytidine/deoxycytidylate deaminase

family protein. Both are expressed in maize kernels, and the *Arabidopsis* homologs AT5G19820 (KETCH1) and AT1G48175 (ATTAD2) are involved in seed embryo development and seed dormancy breaking (Tzafrir *et al.* 2004). *Zm00001d033633*, annotated as a phosphatase, is expressed in the maize seed coat. Its *Arabidopsis* homolog AT2G32150 (XMPP) inhibits the abscisic acid response and promotes seed germination (Lee *et al.* 2022). *Zm00001d033637*, annotated as a GNS1/SUR4 membrane protein family member, encodes a very long chain 3-ketoacyl-CoA synthase. Its *Arabidopsis* homolog AT3G06470 (ELO2) is involved in plant cell wall synthesis and the biosynthesis of ultra-long chain fatty acids, which promotes cell differentiation (Zhou *et al.* 2010). *Zm00001d033640*, annotated as a DUF1764 domain protein, is expressed in maize seeds. Its *Arabidopsis* homolog *AT5G11760* is differentially expressed in response to geminivirus infection and promotes root development during germination (Shida *et al.* 2015). *Zm00001d006753*, annotated as indole-3-acetic (IAA) acid amino acid synthase, catalyzes the formation of IAA-amino acid complexes, so it inhibits auxin signaling and activates disease resistance (Ding *et al.* 2008). *Zm00001d007058*, annotated as Protein Mo25, controls cell growth and proliferation, so it influences organ and body size (Ta *et al.* 2023). *Zm00001d017699*, annotated as probable xyloglucan endotransglycosylase/hydroxylase protein 30, catalyzes xylan endohydrolysis (XEH) and transglycosylation (XET), which influences cell wall growth, small molecule metabolism, and cell salt tolerance (Yan *et al.* 2019). *Zm00001d018954*, annotated as the Rhicadhesin receptor, is involved in bacterial attachment and nitrogen fixation symbiotics in peas (Downie 2010). *Zm00001d045028*, annotated as Nuclear GTP binding protein 1, plays important roles in embryogenesis, leaf and cotyledon development, and establishing leaf polarity (Wang *et al.* 2012).

The GO and KEGG analyses of 47 candidate genes revealed their involvement in acid synthesis and elongation, glycoside metabolism, and root development. Consistent with previous findings, growth and development are considered effective strategies for resisting *A. flavus* infection. In addition, we discovered significant enrichment in the glycoside metabolism pathway, leading us to hypothesize the existence of other mechanisms through which maize counters *A. flavus*. A haplotype analysis of the key genes was conducted to investigate the impact of different haplotypes on resistance. Significant differences in *A. flavus* resistance were observed between the different haplotypes of *Zm00001d033637* and *Zm00001d021197*. Specifically, materials carrying the optimal haplotypes (HapA) of these genes exhibited higher resistance to *A. flavus*. When both genes carried HapA, the resistance was significantly enhanced compared to other haplotypes. This indicates that *Zm00001d033637* and *Zm00001d021197* jointly contribute to *A. flavus* resistance. The use of germplasm with HapA can enhance the resistance of modern cultivated maize varieties. Further analysis revealed that *Zm00001d033637* is involved in fatty acid synthesis, a critical module identified in GO analysis. Fatty acids are essential components of cell membranes, hormones, and other substances, so they play a significant role in pathogen resistance (Zhao *et al.* 2022).

Zm00001d021197 is involved in α-L-fucoside degradation, and α-L-fucosylase is present in maize kernel mucus. Previous studies suggested that maize kernels decompose polysaccharides in the rhizosphere mucus, releasing sugars for microbial utilization and potentially alleviating the stress caused by *A. flavus* (Tsai *et al.* 2017; Pozzo *et al.* 2018; Voiniciuc *et al.* 2018).

4.4. *Zm00001d021197* was selected during the maize domestication and adaptation process

An estimated 1,200 genes have been involved in the process of maize domestication, and these genes affect maize morphological characteristics and adaptability through a variety of mechanisms (Yang *et al.* 2017). Identifying the key genes selected during maize domestication can provide a better understanding of how these genes affect maize morphological characteristics and adaptability. In the process of domestication from teosinte to maize, as well as adaptation from tropical/subtropical maize to temperate maize, we found that the *Zm00001d021197* gene was selected, indicating that this gene had a certain contribution to the adaptability of *A. flavus* resistance. Moreover, bacterial fatty acid metabolites and sugars can trigger plant immune responses (Kutschera *et al.* 2019). However, validation of these findings will require constructing knockout and overexpression mutants of these genes and observing their cellular behavior and changes in resistance to *A. flavus*. This will provide a deeper understanding of the molecular mechanisms underlying maize resistance to *A. flavus* and aid in the development of resistant maize varieties.

4.5. Molecular marker development and application

A pan-genomic sequence comparison revealed an InDel variation in the promoter region of *Zm00001d021197*, and haplotype analysis indicated significant differences in *A. flavus* resistance at this site, despite its absence in the three studied genotypes. A pair of markers targeting this site was developed for the rapid screening of *A. flavus*-resistant materials in breeding programs. A comparison between MY73, Zhengdan 958, and their parental lines suggested that MY73 may exhibit weaker resistance than Zhengdan 958. However, any resistance at additional loci needs to be considered comprehensively, so more markers must be developed to further support the breeding program.

5. Conclusion

In this study, temperate inbreds were found to exhibit stronger resistance to *A. flavus* than tropical and subtropical materials. Thirteen novel QTLs and 47 highly expressed genes were identified using an expanded genotype panel, highlighting the benefits of greater marker density in GWAS. GO and KEGG analyses linked these genes to key processes such as fatty acid synthesis, glycoside decomposition and root development. Among the findings, *ZmAFR16* was identified as a major QTL, with the *Zm00001d021197* gene being pivotal for *A. flavus* resistance, so it is an essential target for modern maize breeding. Notably, this gene was also

selected during the domestication of teosinte (*Zea mays* ssp. *mexicana*) to modern maize, as well as during the adaptation from tropical/subtropical maize to temperate maize. Inbred lines carrying favorable haplotype combinations (HapA for *Zm00001d033637* and HapA for *Zm00001d021197*) exhibited strong resistance to *A. flavus*. Molecular markers were also developed to effectively distinguish maize inbred lines based on *A. flavus* resistance levels. Overall, this study provides crucial insights into the genetic basis of *A. flavus* resistance, which will enhance breeding efficiency for resistant maize varieties.

Acknowledgements

We thank Jianbing Yan's group from Huazhong Agricultural University and Lu Chen's group from Zhejiang University for providing maize genotypic data. This research was financially supported by the National Natural Science Foundation of China (32171980), the China Postdoctoral Science Foundation (2020M682295), the Henan Province Science and Technology Attack Project, China (232102110181, 242102110307), the Natural Science Foundation Youth Fund Project of Henan Province, China (232300421261), and the Henan Provincial Higher Education Key Research Project, China (24B210003).

Declaration of competing interest

The authors declare that they have no conflict of interest.

Declaration of generative AI and AI-assisted technologies in the writing process

During the preparation of this manuscript, the authors used ChatGPT 4.0 to assist in improving the clarity and readability of the language. All content generated was carefully reviewed and revised by the authors as necessary, and the authors take full responsibility for the final content of the article.

Appendices associated with this paper are available at https://doi.org/10.1016/j.jia.2025.01.002

References

Amaike S, Keller N P. 2011. *Aspergillus flavus*. *Annual Review of Phytopathology*, **49**, 107–133.

Ascencio-Ibáñez J T, Sozzani R, Lee T J, Chu T M, Wolfinger R D, Cella R, Hanley-Bowdoin L. 2008. Global analysis of *Arabidopsis* gene expression uncovers a complex array of changes impacting pathogen response and cell cycle during geminivirus infection. *Plant Physiology*, **148**, 436–454.

Baisakh N, Da Silva E A, Pradhan A K, Rajasekaran K. 2023. Comprehensive meta-analysis of QTL and gene expression studies identify candidate genes associated with *Aspergillus flavus* resistance in maize. *Frontiers in Plant Science*, **14**, 1214907.

Brooks T D, Williams W P, Windham G L, Willcox M C, Abbas H K. 2005. Quantitative trait loci contributing resistance to aflatoxin accumulation in the maize inbred Mp313E. *Crop Science*, **45**, 171–174.

Caceres I, Khoury A A, Khoury R E, Lorber S, Oswald I P, Khoury A E, Atoui A, Puel O, Bailly J D. 2020. Aflatoxin biosynthesis and genetic regulation: A review. *Toxins*, **12**, 150.

Chen H, Patterson N, Reich D. 2010. Population differentiation as a test for selective sweeps. *Genome Research*, **20**, 393–402.

Chen L, Luo J, Jin M, Yang N, Liu X, Peng Y, Li W, Phillips A, Cameron B, Bernal J S, Rellán-Álvarez R, Sawers R J H, Liu Q, Yin Y, Ye X, Yan J, Zhang Q, Zhang X, Wu S, Gui S, *et al.* 2022. Genome sequencing reveals evidence of adaptive variation in the genus *Zea*. *Nature Genetics*, **54**, 1736–1745.

Cheng S, Wu T, Zhang H, Sun Z, Mwabulili F, Xie Y, Sun S, Ma W, Li Q, Yang Y, Wu X, Jia H. 2023. Mining lactonase gene from aflatoxin B_1-degrading strain *Bacillus megaterium* and degrading properties of the recombinant enzyme. *Journal of Agricultural and Food Chemistry*, **71**, 20762–20771.

Cogliano V J, Baan R, Straif K, Grosse Y, Lauby-Secretan B, El Ghissassi F, Bouvard V, Benbrahim-Tallaa L, Guha N, Freeman C, Galichet L, Wild C P. 2011. Preventable exposures associated with human cancers. *Journal of the National Cancer Institute*, **103**, 1827–1839.

Ding J. 2016. Analysis of primary mapping of resistance to *Aspergillus flavous* gene and haploid induction and doubling technique in maize. MSc thesis, Anhui Agricultural University, Anhui Province, China. (in Chinese)

Ding X, Cao Y, Huang L, Zhao J, Xu C, Li X, Wang S. 2008. Activation of the indole-3-acetic acid-amido synthetase GH3-8 suppresses expansin expression and promotes salicylate- and jasmonate-independent basal immunity in rice. *The Plant Cell*, **20**, 228–240.

Downie J A. 2010. The roles of extracellular proteins, polysaccharides and signals in the interactions of rhizobia with legume roots. *FEMS Microbiology Reviews*, **34**, 150–170.

Eaton D L, Gallagher E P. 1994. Mechanisms of aflatoxin carcinogenesis. *Annual Review of Pharmacology and Toxicology*, **34**, 135–172.

Erenstein O, Jaleta M, Sonder K, Mottaleb K, Prasanna B M. 2022. Global maize production, consumption and trade: Trends and R&D implications. *Food Security*, **14**, 1295–1319.

Fu H. 2018. *Preventive Medicine*. 7th ed. People's Health Publishing House, Beijing. (in Chinese)

Gui S, Yang L, Li J, Luo J, Xu X, Yuan J, Chen L, Li W, Yang X, Wu S, Li S, Wang Y, Zhu Y, Gao Q, Yang N, Yan J. 2020. ZEAMAP, a comprehensive database adapted to the maize multi-omics era. *iScience*, **23**, 101241.

Han G, Li C, Xiang F, Zhao Q, Zhao Y, Cai R, Cheng B, Wang X, Tao F. 2020. Genome-wide association study leads to novel genetic insights into resistance to *Aspergillus flavus* in maize kernels. *BMC Plant Biology*, **20**, 206.

Hedayati M T, Pasqualotto A C, Warn P A, Bowyer P, Denning D W. 2007. *Aspergillus flavus*: Human pathogen, allergen and mycotoxin producer. *Microbiology-SGM*, **153**, 1677–1692.

Herzallah S, Alshawabkeh K, Fataftah A A. 2008. Aflatoxin decontamination of artificially contaminated feeds by sunlight, γ-radiation, and microwave heating. *Journal of Applied Poultry Research*, **17**, 515–521.

Kato S, Hayashi M, Kitagawa M, Kajiura H, Maeda M, Kimura Y, Igarashi K, Kasahara M, Ishimizu T. 2018. Degradation pathway of plant complex-typeN-glycans: Identification and characterization of a key α1,3-fucosidase from glycoside hydrolase family 29. *The Biochemical Journal*, **475**, 305–317.

Kutschera A, Dawid C, Gisch N, Schmid C, Raasch L, Gerster T, Schäffer M, Smakowska-Luzan E, Belkhadir Y, Vlot A C, Chandler C E, Schellenberger R, Schwudke D, Ernst R K, Dorey S, Hückelhoven R, Hofmann T, Ranf S. 2019. Bacterial medium-chain 3-hydroxy fatty acid metabolites trigger immunity in *Arabidopsis* plants. *Science*, **364**, 178–181.

Lee S, Choi E, Kim T, Hwang J, Lee J H. 2022. AtHAD1, a haloacid dehalogenase-like phosphatase, is involved in repressing the ABA response. *Biochemical and Biophysical Research Communications*, **587**, 119–125.

Li Q, Yang X, Xu S, Cai Y, Zhang D, Han Y, Li L, Zhang Z, Gao S, Li J, Yan J. 2012. Genome-wide association studies identified three independent polymorphisms associated with α-tocopherol content in maize kernels. *PLoS ONE*, **7**, e36807.

Li T, Zhang Z, Wang Y, Li Y, Zhu J, Hu R, Yang Y, Liu M. 2021. Quantitative proteomic analysis for high- and low-aflatoxin-yield *Aspergillus flavus* strains isolated from natural environments. *Frontiers in Microbiology*, **12**, 741875.

Li W, Yu Y, Wang L, Luo Y, Peng Y, Xu Y, Liu X, Wu S, Jian L, Xu J, Xiao Y, Yan J. 2021. The genetic architecture of the dynamic changes in grain moisture in maize. *Plant Biotechnology Journal*, **19**, 1195–1205.

Liu H, Wang F, Xiao Y, Tian Z, Wen W, Zhang X, Chen X, Liu N, Li W, Liu L, Liu J, Yan J, Liu J. 2016. MODEM: Multi-omics data envelopment

and mining in maize. *Database* (Oxford), **2016**, baw117.
Liu Y, Wu F. 2010. Global burden of aflatoxin-induced hepatocellular carcinoma: A risk assessment. *Environmental Health Perspectives*, **118**, 818–824.
Loiselle B A, Sork V L, Nason J, Graham C. 1995. Spatial genetic structure of a tropical understory shrub, *Psychotria Officinalis* (Rubiaceae). *American Journal of Botany*, **82**, 1420–1425.
Nazari M. 2021. Plant mucilage components and their functions in the rhizosphere. *Rhizosphere*, **18**, 100344.
Mideros S X, Warburton M L, Jamann T M, Windham G L, Williams W P, Nelson R J. 2014. Quantitative trait loci influencing mycotoxin contamination of maize: Analysis by linkage mapping, characterization of near-isogenic lines, and meta-analysis. *Crop Science*, **54**, 127–142.
Pozzo T, Higdon S M, Pattathil S, Hahn M G, Bennett A B. 2018. Characterization of novel glycosyl hydrolases discovered by cell wall glycan directed monoclonal antibody screening and metagenome analysis of maize aerial root mucilage. *PLoS ONE*, **13**, e0204525.
Qu L L, Jia Q, Liu C, Wang W, Duan L, Yang G, Han C Q, Li H. 2018. Thin layer chromatography combined with surface-enhanced raman spectroscopy for rapid sensing aflatoxins. *Journal of Chromatography A*, **1579**, 115–120.
Schmidt M A, Mao Y, Opoku J, Mehl H L. 2021. Enzymatic degradation is an effective means to reduce aflatoxin contamination in maize. *BMC Biotechnology*, **21**, 70.
Shida T, Fukuda A, Saito T, Ito H, Kato A. 2015. AtRBP1, which encodes an RNA-binding protein containing RNA-recognition motifs, regulates root growth in *Arabidopsis thaliana*. *Plant Physiology and Biochemistry*, **92**, 62–70.
Shim W B, Yang Z Y, Kim J S, Kim J Y, Kang S J, Woo G J, Chung Y C, Eremin S A, Chung D H. 2007. Development of immunochromatography strip-test using nanocolloidal gold-antibody probe for the rapid detection of aflatoxin B1 in grain and feed samples. *Journal of Microbiology and Biotechnology*, **17**, 1629–1637.
Sözen C, Schenk S T, Boudsocq M, Chardin C, Almeida-Trapp M, Krapp A, Hirt H, Mithöfer A, Colcombet J. 2020. Wounding and insect feeding trigger two independent MAPK pathways with distinct regulation and kinetics. *The Plant Cell*, **32**, 1988–2003.
Ta K N, Yoshida M W, Tezuka T, Shimizu-Sato S, Nosaka-Takahashi M, Toyoda A, Suzuki T, Goshima G, Sato Y. 2023. Control of plant cell growth and proliferation by MO25a, a conserved major component of the mammalian sterile 20-like kinase pathway. *Plant & Cell Physiology*, **64**, 336–351.
Thakare D, Zhang J, Wing R A, Cotty P J, Schmidt M A. 2017. Aflatoxin-free transgenic maize using host-induced gene silencing. *Science Advances*, **3**, e1602382.
de La Torre F, Sampedro J, Zarra I, Revilla G. 2002. AtFXG1, an *Arabidopsis* gene encoding α-L-fucosidase active against fucosylated xyloglucan oligosaccharides. *Plant Physiology*, **128**, 247–255.
Tsai A Y, Kunieda T, Rogalski J, Foster L J, Ellis B E, Haughn G W. 2017. Identification and characterization of *Arabidopsis* seed coat mucilage proteins. *Plant Physiology*, **173**, 1059–1074.
Tzafrir I, Pena-Muralla R, Dickerman A, Berg M, Rogers R, Hutchens S, Sweeney T C, McElver J, Aux G, Patton D, Meinke D. 2004. Identification of genes required for embryo development in *Arabidopsis*. *Plant Physiology*, **135**, 1206–1220.
Voiniciuc C, Engle K A, Günl M, Dieluweit S, Schmidt M H, Yang J Y, Moremen K W, Mohnen D, Usadel B. 2018. Identification of key enzymes for pectin synthesis in seed mucilage. *Plant Physiology*, **178**, 1045–1064.
Walley J W, Sartor R C, Shen Z, Schmitz R J, Wu K J, Urich M A, Nery J R, Smith L G, Schnable J C, Ecker J R, Briggs S P. 2016. Integration of omic networks in a developmental atlas of maize. *Science*, **353**, 814–818.
Wang X, Gingrich D K, Deng Y, Hong Z. 2012. A nucleostemin-like GTPase required for normal apical and floral meristem development in *Arabidopsis*. *Molecular Biology of the Cell*, **23**, 1446–1456.
Wang Y, Dong Y J, Li Z M, Deng L G, Guo C Y, Zhang S Q, Li D P, Zhao S C. 2016. Fast determination of multi-mycotoxins in corn by dispersive solid-phase extraction coupled with ultra-performance liquid chromatography with tandem quadrupole time-of-flight mass spectrometry. *Journal of Integrative Agriculture,* **15**, 1656–1666.
Willcox M C, Davis G L, Warburton M L, Windham G L, Abbas H K, Betrán J, Holland J B, Williams W P. 2013. Confirming quantitative trait loci for aflatoxin resistance from Mp313E in different genetic backgrounds. *Molecular Breeding*, **32**, 15–26.
Xiang K, Zhang Z M, Reid L M, Zhu X Y, Yuan G S, Pan G T. 2010. A meta-analysis of QTL associated with ear rot resistance in maize. *Maydica*, **55**, 281–290.
Yan J, Huang Y, He H, Han T, Di P, Sechet J, Fang L, Liang Y, Scheller H V, Mortimer J C, Ni L, Jiang M, Hou X, Zhang A. 2019. Xyloglucan endotransglucosylase-hydrolase30 negatively affects salt tolerance in *Arabidopsis*. *Journal of Experimental Botany*, **70**, 5495–5506.
Yang N, Liu J, Gao Q, Gui S, Chen L, Yang L, Huang J, Deng T, Luo J, He L, Wang Y, Xu P, Peng Y, Shi Z, Lan L, Ma Z, Yang X, Zhang Q, Bai M, Li S, Li W, Liu L, Jackson D, Yan J. 2019. Genome assembly of a tropical maize inbred line provides insights into structural variation and crop improvement. *Nature Genetics*, **51**, 1052–1059.
Yang N, Xu X W, Wang R R, Peng W L, Cai L, Song J M, Li W, Luo X, Niu L, Wang Y, Jin M, Chen L, Luo J, Deng M, Wang L, Pan Q, Liu F, Jackson D, Yang X, Chen L L, Yan J. 2017. Contributions of *Zea mays* subspecies mexicana haplotypes to modern maize. *Nature Communications*, **8**, 1874.
Yang X, Gao S, Xu S, Zhang Z, Prasanna B M, Lin L, Li J, Yan J. 2011. Characterization of a global germplasm collection and its potential utilization for analysis of complex quantitative traits in maize. *Molecular Breeding*, **28**, 511–526.
Yin L, Zhang H, Tang Z, Xu J, Yin D, Zhang Z, Yuan X, Zhu M, Zhao S, Li X, Liu X. 2021. rMVP: A memory-efficient, visualization-enhanced, and parallel-accelerated tool for genome-wide association study. *Genomics, Proteomics & Bioinformatics*, **19**, 619–628.
Yin Y N, Yan L Y, Jiang J H, Ma Z H. Biological control of aflatoxin contamination of crops. 2008. *Journal of Zhejiang University* (Science B), **9**, 787–792.
Yu J, Hennessy D A, Wu F. 2024. Bt corn and cotton planting may benefit peanut growers by reducing aflatoxin risk. *Plant Biotechnology Journal*, **22**, 3028–3036.
Zhang X, Warburton M L, Setter T, Liu H, Xue Y, Yang N, Yan J, Xiao Y. 2016. Genome-wide association studies of drought-related metabolic changes in maize using an enlarged SNP panel. *Theoretical and Applied Genetics*, **129**, 1449–1463.
Zhao H, Sun Z, Wang J, Huang H, Kocher J P, Wang L. 2014. CrossMap: A versatile tool for coordinate conversion between genome assemblies. *Bioinformatics*, **30**, 1006–1007.
Zhao Z, Fan J, Yang P, Wang Z, Opiyo S O, Mackey D, Xia Y. 2022. Involvement of *Arabidopsis* acyl carrier protein 1 in PAMP-triggered immunity. *Molecular Plant-Microbe Interactions*, **35**, 681–693.
Zhou C, Yin Y, Dam P, Xu Y. 2010. Identification of novel proteins involved in plant cell-wall synthesis based on protein–protein interaction data. *Journal of Proteome Research*, **9**, 5025–5037.